AIP | Applied Physics Letters

Graphene sheets embedded carbon film prepared by electron irradiation in electron cyclotron resonance plasma

Chao Wang, Dongfeng Diao, Xue Fan, and Cheng Chen

Citation: Appl. Phys. Lett. **100**, 231909 (2012); doi: 10.1063/1.4727894
View online: http://dx.doi.org/10.1063/1.4727894
View Table of Contents: http://apl.aip.org/resource/1/APPLAB/v100/i23
Published by the American Institute of Physics.

Graphene sheets embedded carbon film prepared by electron irradiation in electron cyclotron resonance plasma

Chao Wang, Dongfeng Diao,[a] Xue Fan, and Cheng Chen
Key Laboratory of Education Ministry for Modern Design and Rotor-Bearing System, School of Mechanical Engineering, Xi'an Jiaotong University, 710049 Xi'an, China

(Received 19 December 2011; accepted 22 May 2012; published online 7 June 2012)

We used a low energy electron irradiation technique to prepare graphene sheets embedded carbon (GSEC) film based on electron cyclotron resonance plasma. The particular π electronic structure of the GSEC film similar to bilayer graphene was verified by Raman spectra 2*D* band analyzing. The phase transition from amorphous carbon to GSEC was initiated when electron irradiation energy reached 40 eV, and the growth mechanism of GSEC was interpreted as inelastic scattering of low energy electrons. This finding indicates that the GSEC film obtained by low energy electron irradiation can be excepted for widely applications with outstanding electric properties. © *2012 American Institute of Physics*. [http://dx.doi.org/10.1063/1.4727894]

Graphene sheet, consisting of sp^2-bonded carbon atoms arranged in hexagon lattice, has attracted major attentions ever since its unique properties had been discovered.[1–4] In the aim of bringing its outstanding properties into practical application, various pathways were proposed to prepare single layer or multilayer graphene sheets such as mechanical cleavage,[1] splitting nanotubes,[5] and chemical processes.[6] However, the above methods are not suitable for large scale application, since they can only produce irregular graphene chips. There are also attempts on large scale growth of graphene layers,[6–10] but the realizing conditions are too sophisticated, limiting their commercial applications. We also know that single layer graphene is not suitable for digital electronic applications since it has no band gap, whereas bilayer graphene, consisting of two stacked graphene layers, acts more like a semiconductor when immersed in an electric field.[11] Indeed, what practical application requires is not the exact material of graphene, but the particular properties of graphene layers such as high electric conductivity[12] and semiconducting performances.[11] Thus, it is valuable to prepare carbon film with the properties close to graphene through an economic process. This methodology can be a promising solution for taking graphene into practical applications.

Plasma, which can produce high density ions and electrons through the process of gas discharge, is widely utilized for large scale film deposition on various kinds of substrate materials. In traditional applications of plasma assisted film deposition, one always employs ions etching on the film. However, few researches referred to the effect of electrons, and the access to growing graphene sheets through electron irradiation was neglected, although the possibility of this method does exist. In this study, we proposed a low energy electron irradiation technique based on electron cyclotron resonance (ECR) plasma, in which centimeter-scale electron irradiation was realized, and graphene sheets embedded carbon (GSEC) films of 60 nm thickness were prepared with the irradiation energy less than 100 eV. We found that the structural transition from amorphous carbon to GSEC, which also lead to a sudden electrical resistance dropping, depends on the electron irradiation energy. The GSEC structure can be achieved when irradiation energy was above 40 eV. Raman study showed that the π electron state of the GSEC film was similar to that of bilayer graphene by decomposing its 2*D* band. We also interpreted the graphene sheet forming mechanism under electron irradiation.

The GSEC film was grown with an ECR plasma sputtering system in which high density plasma (electron density up to 1.1×10^{10} cm^{-3}) was generated to supply the charged particles for irradiation. The detailed description of the ECR plasma system was reported in our former researches.[13,14] Carbon films were grown at the (100) surface of p-type silicon wafer and the size of the substrate wafer was 2 cm × 2 cm × 0.05 cm. During film deposition, a DC bias voltage V_b was applied onto the substrate, ranging from −100 V to +100 V, and the substrate current density (CD) i_s and temperature T_s were obtained under different V_b. The results are shown in Figure 1(a). The inner Figure 1(b) shows the ECR plasma diagnosis result taken by Langmuir single probe (radius 0.1 mm) in the same plasma conditions.

It is obvious that the changing tendency of i_s and T_s along with V_b contain two main periods. When V_b value is between −100 V and 0 V, i_s value is about 2 mA·cm^{-2} and barely changes; when V_b value is between 0 V and +100 V, i_s value dramatically increases from 2 mA·cm^{-2} to 90 mA·cm^{-2}. Meanwhile, T_s is below 50 °C when V_b is below +20 V and rises to nearly 150 °C when V_b increases to +100 V. The major difference of i_s and T_s values under different V_b indicates that the substrate was irradiated by different kinds of charged particles in the plasma. In fact, the i_s curve shows quite similar aspect to that of the plasma diagnosis result in which ion current and electron current were collected as the changing of scanning voltage. Figure 1 shows that the probe tip CD is about twenty times larger than i_s under same bias voltage. This is due to the material difference, since the electrical conductivity of probe tip (tungsten) is ten times higher than substrate holder (stainless steel), and the silicon wafer is a semiconductor. Particularly, when V_b is +50 V, the substrate

[a]Author to whom correspondence should be addressed. Electronic mail: dfdiao@mail.xjtu.edu.cn.

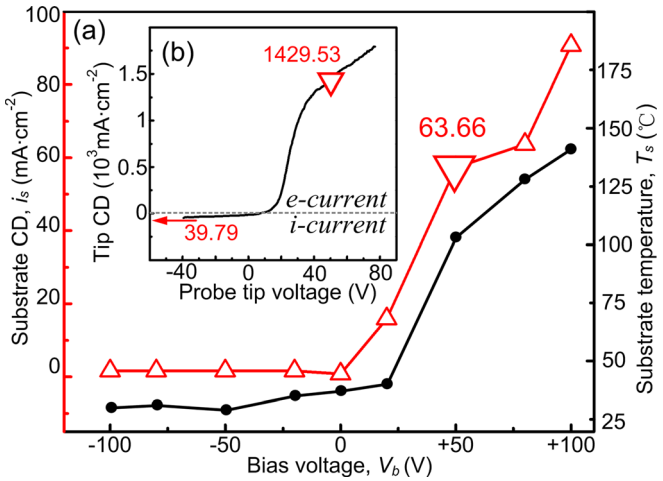

FIG. 1. (a) Substrate CDs i_s and temperature with different bias voltages. Inner figure (b) shows tip CD collected by Langmuir single probe.

CD is 63.66 mA·cm^{-2}, larger than the saturation ion CD 39.79 mA·cm^{-2} (shown in Figure 1(b)). Considering the electrical conductivity difference, the high density current on substrate at V_b of +50 V cannot be formed by ions but only by electrons. Therefore, the electron irradiation can be realized in ECR plasma, and the ion irradiation and electron irradiation can be switched by altering substrate bias voltage.

Carbon films were prepared under electron irradiation and the irradiation energy was from 0 eV to 100 eV, controlled by different bias voltages. The nanostructure of the carbon films were observed with JEOL-2010 TEM and the results are shown in Figure 2.

As shown in the TEM images, the film structures are amorphous-like with the irradiation energy below 50 eV. When irradiation energies are 50 eV, 80 eV, and 100 eV, nano crystallized structure with stacks of graphene sheets appeared in the films and form the GSEC structure. The graphene sheet stacks are distributed uniformly in the amorphous film matrix and grown along random directions. Each stack contains a few graphene layers which are linked with each other by twisting and curving. The distance between two graphene sheets ranges from 0.36 nm to 0.38 nm. The electron diffraction (ED) patterns of GSEC film shows diffraction rings, indicating a more ordered structure than amorphous film.

The bonding structures of carbon films prepared with different electron irradiation energies were studied from their Raman spectra, which were obtained with HORIBA HR800 laser confocal Raman spectrometer. The spot size of 514 nm laser was 2 μm using a 100× objective, and the laser power was kept at 0.1 mW to avoid ample surface heating. The spectrum between 1100 cm^{-1} and 3400 cm^{-1} is shown in Figure 3(a).

When irradiation energies are 0 eV and 20 eV, both two spectra exhibit a composite band centered around 1500 cm^{-1}, consisting of *D* and *G* bands. The absence of *2D* peak in the two spectra indicates that the films are amorphous with no graphitic crystallized structure. As the irradiation energy increases to 40 eV and above, the *D* and *G* bands locate separately near 1340 cm^{-1} and 1600 cm^{-1}, respectively. The GSEC film structure with irradiation energy of 40 eV is detected by Raman spectrum but not in its TEM image. This indicates that the film

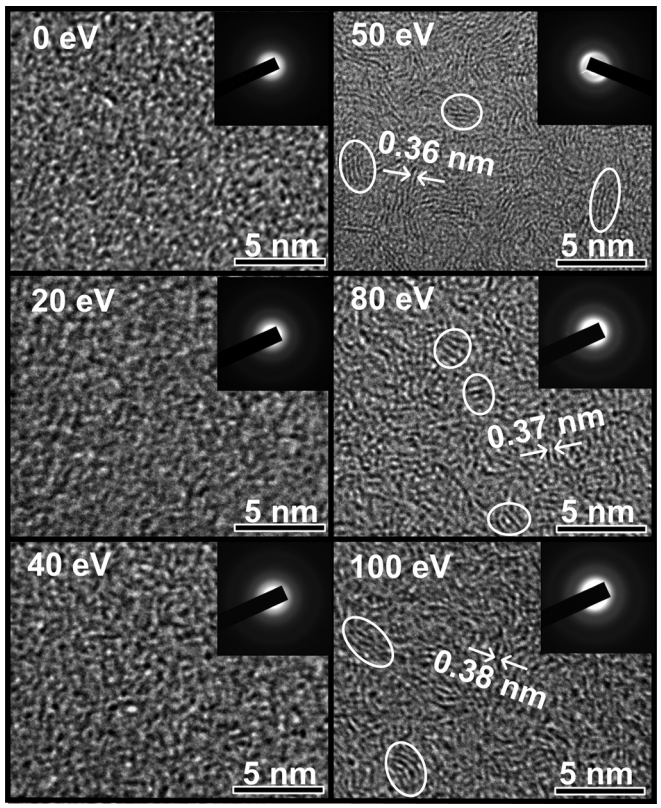

FIG. 2. Top view TEM images of carbon films prepared under electron irradiation with different electron irradiating energies ranging from 0 eV to 100 eV. The GSEC structure can be clearly shown when irradiation energy is larger than 50 eV. The distance between embedded graphene sheets ranges from 0.36 nm to 0.38 nm.

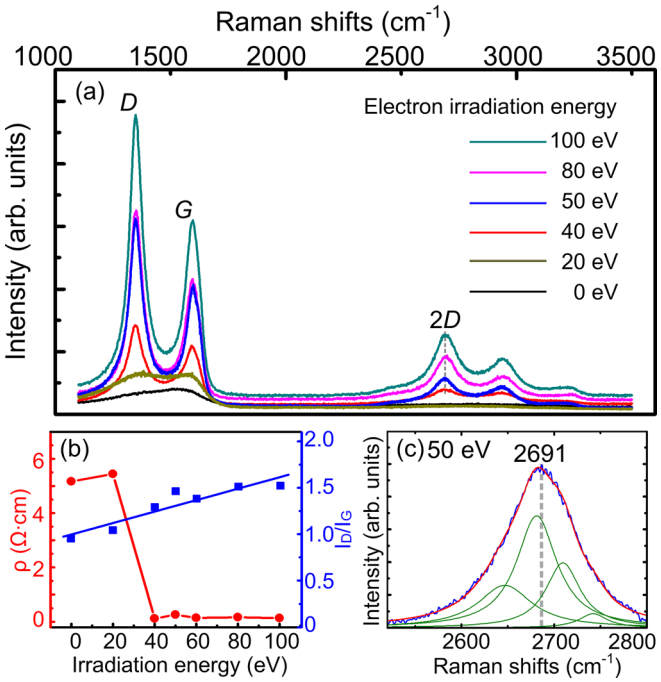

FIG. 3. (a) Raman spectra of carbon films prepared with electron irradiation energies ranged from 0 to 100 eV. (b) The ratios of *D* band to *G* band and the electrical resistances ρ of carbon films (measured by the four-point-probe method at room temperature). (c) Detailed 2*D* band (blue curve) of GSEC film prepared with electron irradiation energy of 50 eV, including the band center at 2691 cm^{-1} (dashed grey line), four Lorentz components (green curves), and the fitting result (red curve).

structure may reach a critical transition state and the graphene sheets start to form, which is difficult to observe by TEM. The ratio of *D* band to *G* band also increased to higher value as shown in Figure 3(b), which indicates the formation of graphitic nano crystallized structure, since *D* band reflects aromatic ring. Figure 3(b) also exhibits the changing tendency of film electrical resistances ρ (measured by the four-point-probe method at room temperature) with the increasing irradiation energy, and ρ notably decreased by one order of magnitude when irradiation energy reached 40 eV. This sudden change suggests a structural transition from amorphous to GSEC, because the embedded graphene sheets are highly conductive structure. Moreover in Figure 3(a), when irradiation energy is over 40 eV, the spectra showed a medium strength 2*D* band centered near 2700 cm^{-1}. This also proves the existence of graphene sheets in GSEC structure. So the sudden dropping of electrical resistance and the appearance of 2*D* band both imply that the electron irradiation energy for structural transition from amorphous to GSEC is 40 eV.

In order to recognize the electronic structure of GSEC film, the 2*D* band in the spectra were decomposed with Lorentz components. Since the film structure does not change much in the irradiation energy range from 40 eV to 100 eV, the 2*D* bands are similar. Hereby, we choose one of the spectra (50 eV) for further discussion, and the details are shown in the inset Figure 3(b), which consists the original 2*D* band (blue curve), the band center (dashed grey line), Lorentz component bands (green curves), and the fitting result (red curve).

Due to Ferrari's and Graf's researches,[15,16] the 2*D* band center position is lower than 2700 cm^{-1} only when graphene sheets consist of no more than five layers. So the 2*D* band center of 2691 cm^{-1} indicates that most of the graphene sheet stacks in GSEC film contain no more than five layers. This is well proved by TEM observation in Figure 2. Notably, there is an interesting result that the 2*D* band was perfectly fitted with four Lorentz components. This is the same with bilayer graphene 2*D* band, as reported by other researchers.[17–19] From theoretical study, these four peaks are due to the splitting of π and π^* bands by the interaction of graphene layers.[15] Therefore, the four component bands illustrate the electronic structure of bilayer graphene, which determines its properties such as electrical conductivity and phonon emission.[20–22] In order to evaluate the four component bands in our research, their relative splitting from average center were measured and the results are shown in Table I.

The table clearly showed that the component band shifting of the GSEC 2*D* band comply well with theoretical and formal experimental results of bilayer graphene. This means that the π electrons in GSEC films are at the same state as in bilayer graphene. Interestingly, the graphene sheets in GSEC films are perpendicular to the substrate, while the reported bilayer graphene is grown parallel to the substrate. This different orientation allows GSEC film to bring the graphene-like electric properties into 3 dimensional devices since the film can be really thick.

TABLE I. Relative splitting of 2*D* components (cm^{-1}).

Component band center	2647	2680	2708	2740
Shifting	−44	−11	+17	+49
Ferrari's work[a]	−44	−10	+10	+25
Theory[b]	−44	−11	+11	+41

[a]The results of Ferrari's work, see Ref. 15.
[b]The theoretical results, see Ref. 16.

We also notice that the 2*D* band becomes stronger with the increment of irradiation energy, indicating the increasing content of embedded graphene sheets in the film. Meanwhile, the 2*D* band center and its shape hardly changes. This signifies that the graphene sheets in these films still exist in the form of few layered stacks, instead of bulk layered graphite. The electron diffraction study also proved this information.

In order to understand the GSEC film formation mechanism under low energy electron irradiation in ECR plasma, we propose a description on this subject, which is illustrated in Figure 4. Figure 4(a) was simplified to emphasize the formation of electron irradiation. Electrons are resonantly accelerated to move around the magnetic field lines, and their momentum at the magnetic mirror position (dashed lines in Figure 4(a)) is zero.[14] By taking advantage of this characteristic of ECR plasma, we developed the low energy electron irradiation technique: A positive bias voltage V_b is applied on substrate, which is located nearby the magnetic mirror position. Electrons gain kinetic energy from V_b and irradiate the film, forming substrate current i_s. Meanwhile, the Ar^+ ions are attracted to the carbon target and sputtered the target surface, providing the carbon atoms for film growth.

The electron-atom-interaction is shown in Figure 4(b). Low energy (less than 100 eV) electrons exchange energy with valence electrons of carbon atoms through inelastic scattering (dashed line), and the hybridization change from sp^3 (dark green) to sp^2 (light green) is induced. This is different from the ion irradiation mechanism, in which the inelastic collision between impacting ions and atom nuclei is mainly considered.[23,24] During one inelastic scattering process of irradiating electron, its kinetic energy is lost through several means (electron excitation, plasmon excitation, phonon excitation, etc.). When the energy loss is large enough, one part of it ΔE can trigger the hybridization change of carbon atom by breaking a *C-C* bond (bond energy of 3.6 eV) in sp^3 system. According to our calculations based on electron inelastic scattering in carbon base,[25,26] the electron energy loss per inelastic process increases with its irradiation energy nonlinearly. When irradiation energy rises from 20 eV to 40 eV, the electron energy loss increased from 4.2 eV to

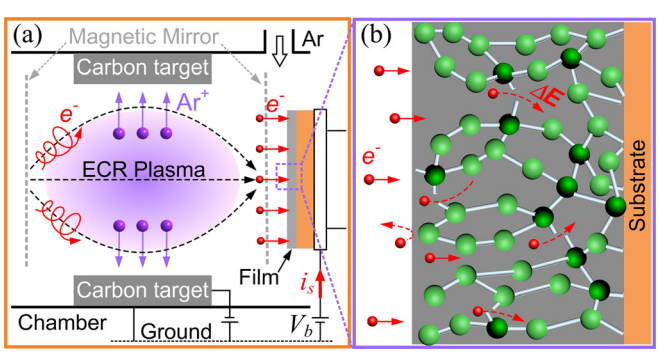

FIG. 4. Illustration of graphene sheets forming under electron irradiation. (a) Electron irradiation formation in ECR plasma; (b) electron-atom-interaction. sp^2 C atoms are in light green and sp^3 C atoms are in dark green.

17.1 eV. This dramatic increasing is essential for breaking the *C-C* bond to form sp^2 hybridization. We also characterized the film binding configuration with x-ray photoelectron spectra, and the sp^2 content increased as the structural transition took place. There are some researches on graphitic structure formation in amorphous carbon by high energy electron beam in TEM,[27–29] and high energy electron beam irradiation for nano structure modification.[30,31] However, these methods were unapplicable for large scale graphene preparation, and the electron beam energy was much higher than in our study.

One thing should be noticed that the irradiating electrons also attribute to higher temperature of the film substrate (Figure 1). In our study, the substrate temperature under electron irradiation increased from 21 °C to below 150 °C, which was measured by a thermal meter behind the substrate surface. This is another clue that the graphene sheets were formed by electron irradiation, since the substrate temperature of higher than 250 °C was indispensable to form graphene sheets in ion irradiation.[32]

In conclusion, we proposed an ECR plasma-based low energy electron irradiation technique. By using this technique, the carbon film structural transition from amorphous to GSEC was found with the irradiation energy of 40 eV. The GSEC film shows similar π electronic structure with that of bilayer graphene, which was verified by analyzing its 2*D* band in Raman spectrum. Comparing with mechanical cleavage and epitaxial growth, the most commonly used methods to obtain few layer graphenes, the low energy electron irradiation technique is high efficiency and economical. This finding indicates that the GSEC film can be expected for broad applications in many fields such as electronics and nanomachinery.

The authors thank the National Nature Science Foundation of China under Grant Number of 90923027. The authors also wish to thank Dr. S. Hirono for helpful discussion.

[1]K. S. Novoselov, A. K. Geim, S. V. Morozov, D. Jiang, Y. Zhang, S. V. Dubonos, I. V. Grigorieva, and A. A. Firsov, Science **306**, 666 (2004).
[2]Y. B. Zhang, Y. W. Tan, H. L. Stormer, and P. Kim, Nature **438**, 201 (2005).
[3]A. K. Geim and K. S. Novoselov, Nature Mater. **6**, 183 (2007).
[4]K. S. Novoselov, A. K. Geim, S. V. Morozov, D. Jiang, M. I. Katsnelson, I. V. Grigorieva, S. V. Dubonos, and A. A. Firsov, Nature **438**, 197 (2005).
[5]L. Jiao, L. Zhang, X. Wang, G. Diankov, and H. Dai, Nature **458**, 877 (2009).
[6]X. Li, X. Wang, L. Zhang, S. Lee, and H. Dai, Science **319**, 1229 (2008).
[7]P. W. Sutter, J. Flege, and E. Sutter, Nature Mater. **7**, 406 (2008).
[8]C. Berger, Z. Song, X. Li, X. Wu, N. Brown, C. Naud, D. Mayou, T. Li, J. Hass, A. N. Marchenkov, E. H. Conrad, P. N. First, and W. A. Heer, Science **312**, 1191 (2006).
[9]K. S. Kim, Y. Zhao, H. Jang, S. Y. Lee, J. M. Kim, K. S. Kim, J. H. Ahn, P. Kim, J. Y. Choi, and B. H. Hong, Nature **457**, 706 (2009).
[10]Y. Pan, H. Zhang, D. Shi, J. Sun, S. Du, F. Liu, and H. Gao, Adv. Mater. **21**, 2777 (2009).
[11]K. S. Novoselov, E. McCann, S. V. Morozov, V. I. Fal'ko, M. I. Katsnelson, U. Zeitler, D. Jiang, F. Schedin, and A. K. Geim, Nat. Phys. **2**, 177 (2006).
[12]S. Hirono, S. Umemura, M. Tomita, and R. Kaneko, Appl. Phys. Lett. **80**, 425 (2002).
[13]C. Wang and D. Diao, Surf. Coat. Technol. **206**, 1899 (2011).
[14]X. Fan, D. Diao, K. Wang, and C. Wang, Surf. Coat. Technol. **206**, 1963 (2011).
[15]A. C. Ferrari, J. C. Meyer, V. Scardaci, C. Casiraghi, M. Lazzeri, F. Mauri, S. Piscanec, D. Jiang, K. S. Novoselov, S. Roth, and A. K. Geim, Phys. Rev. Lett. **97**, 187401 (2006).
[16]D. Graf, F. Molitor, K. Ensslin, C. Stampfer, A. Jungen, C. Hierold, and L. Wirtz, Nano Lett. **7**, 238 (2007).
[17]A. C. Ferrari, Solid State Commun. **143**, 47 (2007).
[18]E. B. Song, B. Lian, G. Xu, B. Yuan, C. Zeng, A. Chen, M. Wang, S. Kim, M. Lang, Y. Zhou, and K. L. Wang, Appl. Phys. Lett. **96**, 081911 (2010).
[19]M. Okano, R. Matsunaga, K. Matsuda, S. Masubuchi, T. Machida, and Y. Kanemitsu, Appl. Phys. Lett. **99**, 151916 (2011).
[20]Z. M. Liao, B. H. Han, H. C. Wu, and D. P. Yu, Appl. Phys. Lett. **97**, 163110 (2010).
[21]A. S. Nunez, E. S. Morell, and P. Vargas, Appl. Phys. Lett. **98**, 262107 (2011).
[22]T. Limmer, A. J. Houtepen, A. Niggebaum, R. Tautz, and E. Da Como1, Appl. Phys. Lett. **99**, 103104 (2011).
[23]M. Chhowalla, J. Robertson, C. W. Chen, S. R. P. Silva, C. A. Davis, G. A. J. Amaratunga, and W. I. Milne, J. Appl. Phys. **81**, 139 (1997).
[24]J. Robertson, Mater. Sci. Eng. R. **37**, 129 (2002).
[25]S. Tanuma, C. J. Powell, and D. R. Penn, J. Appl. Phys. **103**, 063707 (2009).
[26]S. Tanuma, C. J. Powell, and D. R. Penn, Surf. Interface Anal. **43**, 689 (2011).
[27]D. Ugarte, Nature **359**, 707 (1992).
[28]B. S. Xu and S. I. Tanaka, Acta Mater. **46**, 5249 (1998).
[29]S. Aikawa, T. Kizu, and E. Nishikawa, Carbon **48**, 2989 (2010).
[30]J. Zang, L. Bao, R. A. Webb, and X. Li, Nano Lett. **11**, 4885 (2011).
[31]E. Cruz-Silva, A. R. Botello-Mendez, Z. M. Barnett, X. Jia, M. S. Dresselhaus, H. Terrones, M. Terrones, B. G. Sumpter, and V. Meunier, Phys. Rev. Lett. **105**, 045501 (2010).
[32]M. Chhowalla, A. C. Ferrari, J. Robertson, and G. A. J. Amaratunga, Appl. Phys. Lett. **76**, 1419 (2000).